Isogeometric Collocation Analysis

Modeling of Continuous Robots using Shape Functions

Philipp T. Tempel

Laboratoire des Sciences du Numérique de Nantes (LS2N)

January 25, 2021

Section 1

Problem Statement

Problem Statement

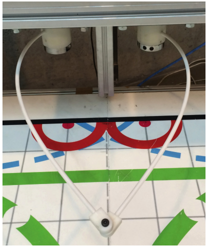

Figure: Altuzarra *et al.*: "Kinematic Characteristics of Parallel Continuum Mechanisms" (2019)

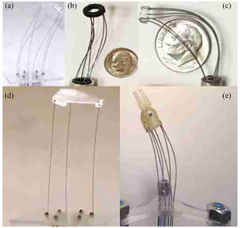

Figure: Black *et al.*: "Parallel Continuum Robots" (2018)

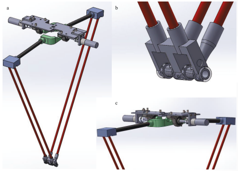

Figure: Campa *et al.*: "A 2 Dof Continuum Parallel Robot for Pick & Place Collaborative Tasks" (2019)

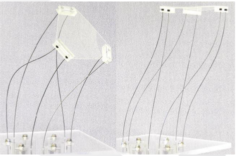

Figure: Till *et al.*: "Elastic Stability of Cosserat Rods and Parallel Continuum Robots" (2017)

Kinematics, dynamics, control, design are very dependent on how the slender structure's large displacements and deformations are described.

Contents

Section 2

Modeling

Configuration of the Rod

Modeling

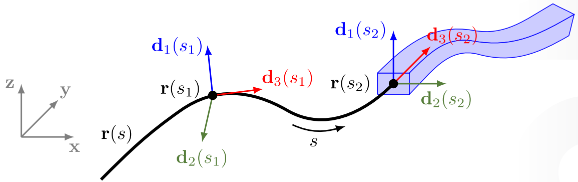

Consider the slender structure to be a *framed curve* of length L. It is represented by the line of its mass centroids, its *centerline*, a spatial curve

$$\boldsymbol{p} \colon [0, L] \to \mathbb{R}^3 \,.$$

A *frame* i.e., a local orthonormal basis field describes the *evolution of the orientation* of the cross-sections

$$\begin{aligned} &\boldsymbol{R} \colon [0, L] \to \mathrm{SO}(3) \,, \\ &\quad \boldsymbol{R}(s) = \left[\boldsymbol{d}_1(s), \quad \boldsymbol{d}_2(s), \quad \boldsymbol{d}_3(s)\right] \in \mathbb{R}^{3\times 3} \,, \\ &\quad \boldsymbol{R}^\top \boldsymbol{R} = \mathbb{I} \,, \\ &\quad \det \boldsymbol{R} = 1 \; \forall s \in [0, L] \end{aligned}$$

Parametrization of the Rotation

Modeling

Commonly, Cosserad rod theory use quaternions for the parametrization of the rotation matrix, though other options exist i.e., Euler angles, rotation vectors, or axis angle.
Let

$$\boldsymbol{q} = \begin{bmatrix} q_1 \\ q_2 \\ q_3 \\ q_4 \end{bmatrix} = \begin{bmatrix} q_s \\ \boldsymbol{q}_v \end{bmatrix} \in \mathbb{R}^4 \, ,$$

be a proper quaternion i.e., $\|\boldsymbol{q}\| = 1$. Its respective rotation matrix reads

$$\boldsymbol{R}(\boldsymbol{q}) = \begin{bmatrix} q_1^2 + q_2^2 - q_3^2 - q_4^2 & 2\,(q_2 q_3 - q_1 q_4) & 2(q_2 q_4 + q_1 q_3) \\ 2(q_2 q_3 + q_1 q_4) & q_1^2 - q_2^2 + q_3^2 - q_4^2 & 2,(q_3 q_4 - q_1 q_2) \\ 2(q_2 q_4 - q_1 q_3) & 2(q_3 q_4 + q_1 q_2) & q_1^2 - q_2^2 - q_3^2 + q_4^2 \end{bmatrix} = \begin{bmatrix} \boldsymbol{d}_1, & \boldsymbol{d}_2, & \boldsymbol{d}_3 \end{bmatrix} .$$

Kinematics and Constitutive Equations

Modeling

Linear strain is defined by the vector

$$\boldsymbol{\varepsilon} = \boldsymbol{R}^\top \boldsymbol{p}' - \hat{\boldsymbol{e}}_3 \,.$$

Angular strain is given as

$$\boldsymbol{\kappa} = \begin{bmatrix} \langle \boldsymbol{d}_2', \boldsymbol{d}_3 \rangle \\ \langle \boldsymbol{d}_3', \boldsymbol{d}_1 \rangle \\ \langle \boldsymbol{d}_1', \boldsymbol{d}_2 \rangle \end{bmatrix} \,.$$

Linear stresses then read

$$\boldsymbol{\sigma} = \boldsymbol{K}_{\text{SE}} \left(\boldsymbol{\varepsilon} - \boldsymbol{\varepsilon}_0 \right) .$$

Angular stresses then read

$$\boldsymbol{\chi} = \boldsymbol{K}_{\text{BT}} \left(\boldsymbol{\kappa} - \boldsymbol{\kappa}_0 \right) .$$

Internal forces of the rod read

$$\boldsymbol{n} = \boldsymbol{R}\,\boldsymbol{\sigma} = \boldsymbol{R}\,\boldsymbol{K}_{\text{SE}} (\boldsymbol{\varepsilon} - \boldsymbol{\varepsilon}_0) \,.$$

Internal moments of the rod read

$$\boldsymbol{m} = \boldsymbol{R}\,\boldsymbol{\chi} = \boldsymbol{R}\,\boldsymbol{K}_{\text{BT}} (\boldsymbol{\kappa} - \boldsymbol{\kappa}_0) \,.$$

Boundary Conditions

Modeling

Usually, the rod is part of a multibody structure and we are interested in the rods constrained kinematic response to the external bodies.

Dirichlet-type condition enforces position and orientation equilibrium at the boundary:

$$\begin{aligned} \boldsymbol{p} - \overline{\boldsymbol{p}} &= \mathbb{0}\,, & s &= 0, L\,, \\ \boldsymbol{q} - \overline{\boldsymbol{q}} &= \mathbb{0}\,, & s &= 0, L\,. \end{aligned}$$

Neumann-type condition enforces force and moment equilibrium at the boundary:

$$\begin{aligned} \boldsymbol{n} - \overline{\boldsymbol{n}} &= \mathbb{0}\,, & s &= 0, L\,, \\ \boldsymbol{m} - \overline{\boldsymbol{m}} &= \mathbb{0}\,, & s &= 0, L\,, \\ \langle \boldsymbol{q}, \boldsymbol{q} \rangle - 1 &= 0\,, & s &= 0, L\,, \end{aligned}$$

Cosserat Model

Modeling

Equilibrium of linear momentum reads

$$\boldsymbol{n}' + \hat{\boldsymbol{n}} = \mathbb{O}\ \forall s \in]0, L[\,,$$

Equilibrium of angular momentum reads

$$\boldsymbol{m}' + \boldsymbol{p}' \times \boldsymbol{n} + \hat{\boldsymbol{m}} = \mathbb{O}\ \forall s \in]0, L[\,,$$

Given an initial condition of the rod

$$\boldsymbol{p}(s=0) = \boldsymbol{p}_0\,,$$
$$\boldsymbol{q}(s=0) = \boldsymbol{q}_0\,,$$
$$\boldsymbol{n}(s=0) = \boldsymbol{n}_0\,,$$
$$\boldsymbol{m}(s=0) = \boldsymbol{m}_0\,,$$

The Cosserat model for flexible slender strutures reads

$$\boldsymbol{p}' = \boldsymbol{R}\left(\boldsymbol{K}_{\mathrm{SE}}{}^{-1}\boldsymbol{R}^\top \boldsymbol{n} + \varepsilon_0\right)$$
$$\boldsymbol{q}' = \begin{bmatrix} 0 \\ \boldsymbol{R}\left(\boldsymbol{K}_{\mathrm{BT}}{}^{-1}\boldsymbol{R}^\top \boldsymbol{m} + \kappa_0\right)\end{bmatrix} \odot \boldsymbol{q}\,,$$
$$\boldsymbol{n}' = -\hat{\boldsymbol{n}}\,,$$
$$\boldsymbol{m}' = -\boldsymbol{p}' \times \boldsymbol{n} - \hat{\boldsymbol{m}}\,.$$

Section 3

Solving

Overview

Solving

In general, the evolution of the Cosserat rod position and orientation is a coupled differential equation in $\mathbb{R}^{13}$ unknowns

$$\boldsymbol{y}' = \boldsymbol{f}(\boldsymbol{y}) , \qquad \boldsymbol{y}^\top = \left[\boldsymbol{p}^\top, \boldsymbol{q}^\top, \boldsymbol{n}^\top, \boldsymbol{m}^\top\right] .$$

Due to the coupled nature e.g., $\boldsymbol{m}' = \boldsymbol{m}'(\boldsymbol{p}', \boldsymbol{n})$, analytical solutions are seldomly obtained. Other methods must be found to obtain the solution for a given initial condition or boundary conditions:

1. Numerical integration
2. Discretization

Numerical Integration

Solving

- Numerical integration is cumbersome and prone to instabilities due to the stiff system
  - High elastic modulus vs. small moment of area
- With combined boundary conditions e.g., positon and orientation at $s = 0$ and forces and moments at $s = L$, numerical integration becomes even more cumbersome
  - Consider problem as BVP rather than IVP then
- When considering dynamics and optimization, numerical integration is impractical
- Other quantities of interest are not easily obtainable e.g., linearization, mass-matrix, stiffness, etc.

Discretization: The CoRdE Approach

Solving

Let us discretize the centerline $\boldsymbol{p}$ as a chain of N nodes $\boldsymbol{p}_i$, the quaternions as a chain of $N-1$ nodes $\boldsymbol{q}_j$. The discrete spatial derivative $\boldsymbol{y}'$ ($\boldsymbol{y} \equiv \boldsymbol{p}$ or $\boldsymbol{y} \equiv \boldsymbol{q}$) reads

$$\boldsymbol{y}_i' = \frac{\boldsymbol{y}_{i+1} - \boldsymbol{y}_i}{\|\boldsymbol{y}_{i+1} - \boldsymbol{y}_i\|} \,.$$

With high stretch stiffness, it can be approximated to be

$$\boldsymbol{p}_i' \approx \frac{1}{L_i}(\boldsymbol{p}_{i+1} - \boldsymbol{p}_i)\,, \qquad \boldsymbol{q}_i' \approx \frac{1}{L_i}(\boldsymbol{q}_{i+1} - \boldsymbol{q}_i)\,.$$

In the end, we obtain a high-dimensional system of nonlinear equations in $\boldsymbol{p}_i$, $i = 1, \dots, N$ and $\boldsymbol{q}_j$, $j = 1, \dots, N-1$. It provides a linear approximation of the rod's centerline and orientation, particularly a linear approximation between nodes.

Discretization: The Shape Function Approach

Solving

Let us *discretize* the centerline position and quaternion using (for now) n unknown *shape functions* $\Pi_i(s)$, $i = 1, \ldots, n$

$$\boldsymbol{p}(s) = \sum_i^n \Pi_i(s)\, \boldsymbol{p}_i = \boldsymbol{\Pi}(s)\, \boldsymbol{P}_{\boldsymbol{p}}\,, \qquad \boldsymbol{q}(s) = \sum_i^n \Pi_i(s)\, \boldsymbol{q}_i = \boldsymbol{\Pi}(s)\, \boldsymbol{P}_{\boldsymbol{q}}\,.$$

This is similar to a modal decomposition or linear coordinate transformation where we introduce new generalized coordinates $\boldsymbol{P}_{\boldsymbol{y}}$ for the sought-for physical properties.
We have not made any assumptions as to what $\boldsymbol{\Pi}(u)$ shall look like, so let us take a look at (one particular) literature.

Section 4

Isogeometric Analysis

Introduction

Isogeometric Analysis

Isogeometric Analysis Hughes, Cottrell, and Bazilevs

Based on the isogeometric philosophy, the solution space for dependent variables is represented in terms of the same functions which represent geometry [5].

- A new method for the analysis of problems governed by partial differential equations e.g., solids, structures, and fluids.
- Many features in common with finite element method and some with meshless methods
- Purely based on geometric propertyes and inspired from CAD
- Approach is based on NURBS (Non-Uniform Rational B-Splines), a standard technology in CAD systems

B-Splines

Isogeometric Analysis

A *knot vector* is a set of coordinates in the parametric space

$$\Xi = \{\xi_1, \xi_2, \dots, \xi_{n+p+1}\},$$

which the i-th knot $\xi_i \in \mathbb{R}$, p is the polynomial order ($p = d + 1$), and n is the number of bases functions.

B-Splines are defined recursively starting with piecewise constants ($p = 0$):

$$N_{i,0}(u) = \begin{cases} 1 & \text{if } \xi_i \le u < \xi_{i+1}, \\ 0 & \text{otherwise} \end{cases}.$$

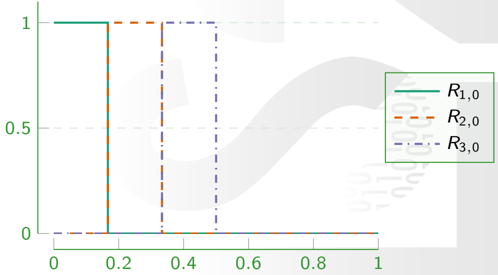

B-Splines

Isogeometric Analysis

For $p = 1, 2, \ldots,$ we have

$$N_{i,p}(u) = \frac{u - \xi_i}{\xi_{i+p} - \xi_i} N_{i,p-1}(u) + \frac{\xi_{i+p+1} - u}{\xi_{i+p+1} - \xi_{i+1}} N_{i+1,p-1}(u)$$

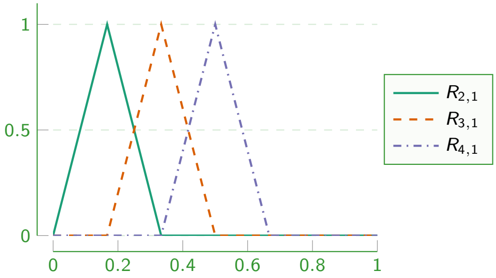

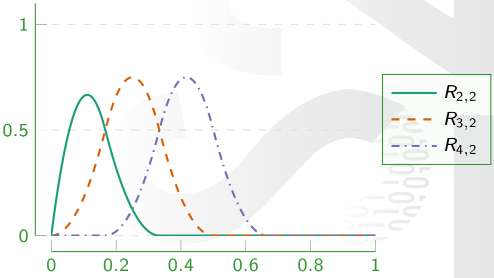

B-Splines

Isogeometric Analysis

A few important properties of B-Splines:

1. Basis functions of order p are $p-1$ continuous
2. B-Splines constitute a partition of unity i.e., $\sum_{i=1}^{n} N_{i,p}(u) = 1$.
3. Each $N_{i,p}$ has only compact support and is contained in the interval $[\xi_i, \xi_{i+p+1}]$.
4. Each basis function is non-negative consequently all coefficients of the mass matrix computed from B-Splines are greater than or equal to zero.
5. Basis functions are interpolating at the ends of the parametric space $[\xi_1, \xi_{n+p+1}]$ but not, in general, at the interior knots (where they are, in fact, approximating).

Curves: B-Spline

Isogeometric Analysis

B-Spline curves in $\mathbb{R}^m$ are a linear combination of B-Spline basis functions

$$\boldsymbol{C}(u) = \sum_{i=1}^{k} N_{i,p}(u)\, \boldsymbol{P}_i\, .$$

Table: Control points of sample curve with $p = 3$.

i	1	2	3	4	5	6
$\boldsymbol{P}_{i,x}$	0	0.3	0.3	0.5	0.9	0.8
$\boldsymbol{P}_{i,y}$	0	0.25	0.7	0.8	0.3	1

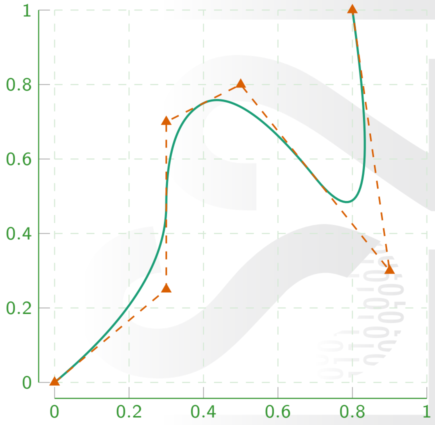

Curves: NURBS

Isogeometric Analysis

NURBS (Non-Uniform Rational B-Splines) are a projective transformation of B-Spline curves

$$\boldsymbol{C}(u) = \sum_{i=1}^{k} \frac{N_{i,p}(u) w_i}{\sum_{j=1}^{k} N_{j,p}(u) w_j} \boldsymbol{P}_i \,,$$

Table: Control points of sample curves.

i	1	2	3	4	5	6
$\boldsymbol{P}_{i,x}$	0	0.3	0.3	0.5	0.9	0.8
$\boldsymbol{P}_{i,y}$	0	0.25	0.7	0.8	0.3	1
w_i	1	1	1	1	1	1
$\boldsymbol{P}_{i,x}$	0	1.5	0.3	0.5	0.9	0.8
$\boldsymbol{P}_{i,y}$	0	1.25	0.7	0.8	0.3	1
w_i	1	5	1	1	1	1

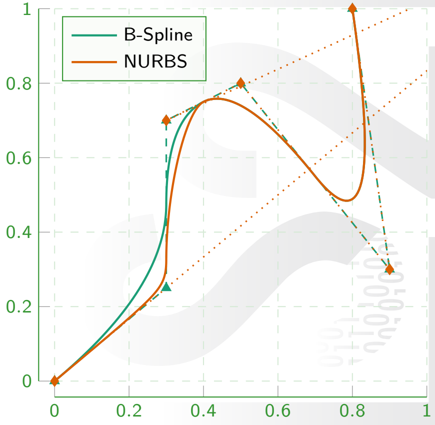

Curves: Properties

Isogeometric Analysis

A few additional properties of B-Spline and NURBS curves

1. Polynomial order may be increased (p-refinement) *without* changing the geometry of parametrization
2. *Affine transformations* in physical space are *obtained* by applying the transformation to the *control points* (NURBS possess affine covariance).

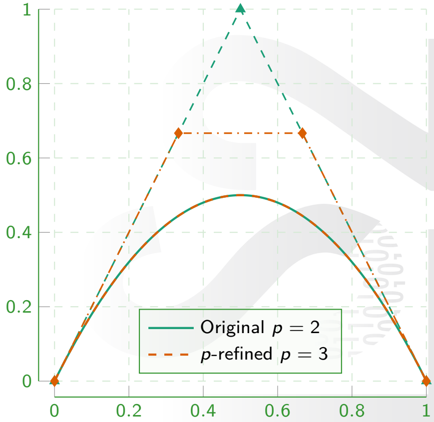

Curves: Approximation of circle

Isogeometric Analysis

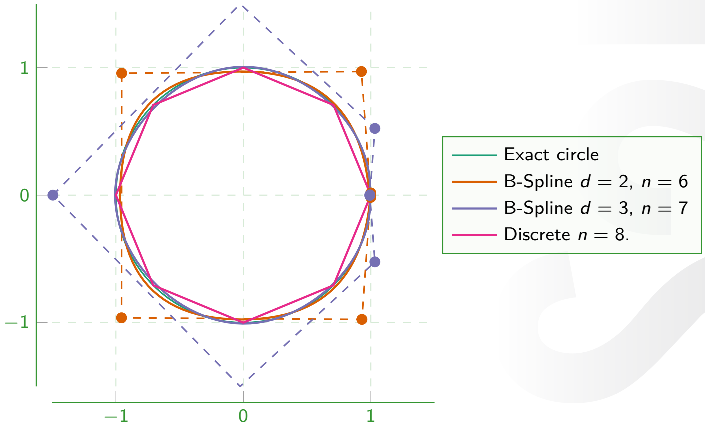

Isogeometric Rod

Isogeometric Analysis

Let us *discretize* the centerline position and quaternion using n NURBS as *shape functions* $\Pi_i(s)$, $i = 1, \ldots, n$:

$$\boldsymbol{p}(s) = \sum_i^n \Pi_i(s)\, \boldsymbol{p}_i = \boldsymbol{\Pi}(s)\, \boldsymbol{P}_{\boldsymbol{p}} \ , \qquad \boldsymbol{q}(s) = \sum_i^n \Pi_i(s)\, \boldsymbol{q}_i = \boldsymbol{\Pi}(s)\, \boldsymbol{P}_{\boldsymbol{q}} \ .$$

Strain measures

$$\boldsymbol{\varepsilon} = \boldsymbol{R}^\top \boldsymbol{p}' - \hat{\boldsymbol{e}}_3 \ ,$$

$$\boldsymbol{\kappa} = \begin{bmatrix} \langle \boldsymbol{d}_2', \boldsymbol{d}_3 \rangle \\ \langle \boldsymbol{d}_3', \boldsymbol{d}_1 \rangle \\ \langle \boldsymbol{d}_1', \boldsymbol{d}_2 \rangle \end{bmatrix} \ .$$

Internal forces

$$\boldsymbol{n} = \boldsymbol{R}\, \boldsymbol{\sigma} = \boldsymbol{R}\, \boldsymbol{K}_{\text{SE}}(\boldsymbol{\varepsilon} - \boldsymbol{\varepsilon}_0) \ ,$$

$$\boldsymbol{m} = \boldsymbol{R}\, \boldsymbol{\chi} = \boldsymbol{R}\, \boldsymbol{K}_{\text{BT}}(\boldsymbol{\kappa} - \boldsymbol{\kappa}_0) \ .$$

Equilibrium equations

$$\boldsymbol{n}' + \hat{\boldsymbol{n}} = \mathbb{O} \ ,$$

$$\boldsymbol{m}' + \boldsymbol{p}' \times \boldsymbol{n} + \hat{\boldsymbol{m}} = \mathbb{O} \ .$$

Substituting the *discrete* centerline position and quaternion into the kinematics simply *transforms* into another solution space. There is *no gain* from this, so we want to also *solve* the *equilibrium equations* in a different way.

Section 5

Collocation

Derivation

Collocation

Let us construct a *one-step method* of given order of accuracy for the *first time step interval* $[t_0, t_0 + h]$. Let $0 \leq c_1 < c_2 < \cdots < c_s \leq 1$ be *distinct nodes* on the unit interval. The *collocation polynomial* $u(t) \in \mathbb{R}^n$ is a polynomial of degree s satisfying

$$u(t_0) = y_0$$
$$u'(t_0 + c_i\, h) = f(u(t_0 + c_i\, h)) \qquad i = 1, \ldots, s\,,$$

and the numerical solution of the *collocation method* over the interval $[t_0, t_0 + h]$ is given by $y_1 = u(t_0 + h)$.

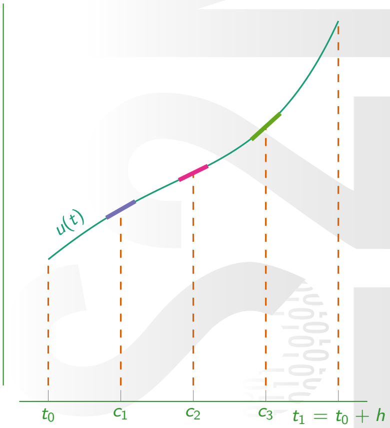

We *construct a polynomial* that passes through y_0 and *agrees with the ODE* at s nodes on $[t_0, t_0 + h]$.

Derivation

Collocation

Let F_i, $i = 1, \ldots, s$, be the values of the (as of yet undetermined) *interpolating polynomial* at the nodes

$$F_i := u'(t_0 + c_i\, h)\,.$$

We use *Lagrange's interpolation formula* to define the polynomial $u'(t)$ passing through these points

$$u'(t) = \sum_{i=1}^{s} F_i\, l_i\left(\frac{t - t_0}{h}\right)\,, \quad l_i(x) = \prod_{\substack{j=1 \\ j \neq i}}^{s} \frac{x - c_j}{c_i - c_j}\,.$$

Integrating over the intervals $[0, c_i]$ gives

$$u(t_0 + c_i\, h) = y_0 + h \sum_{j=1}^{s} F_j \int_0^{c_i} l_j(x)\, \mathrm{d}x\,.$$

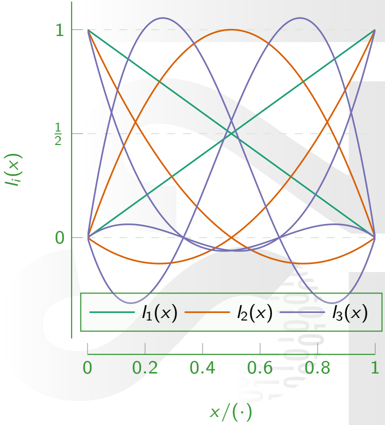

A Simple Example

Collocation

For illustration, let us solve the IVP on the interval $t \in [0, 1]$

$$y' = 3\,t^2\,, \qquad y(0) = 1\,.$$

The exact solution is

$$\tilde{y}(t) = 1 + t^3\,,$$

which we want to approximate with the first-degree polynomial

$$y(t) = a_0 + a_1\,t\,.$$

Since $y(0) = 1$, $a_0 = 1$, substituting gives $a_1 = 3\,t^2$. Requiring the collocation satisfied at $t = 0.5$ gives $a_1 = 0.75$ yields

$$y(t) = 1 + 0.75\,t\,.$$

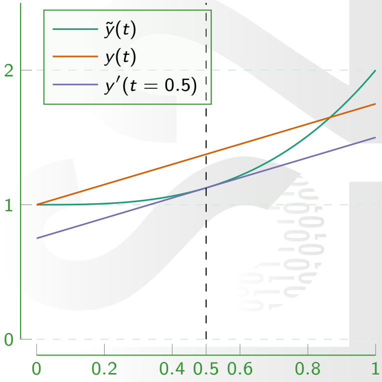

A More Detailed Example

Collocation

Let our IVP be given

$$y' = 1.75\,\exp(1.75\,t)\,, \qquad y(0) = 1.5\,.$$

Our *collocation polynomial* shall be

$$u(t) = a_0 + a_1\,t + a_2\,t^2 + \cdots + a_d\,t^d\,.$$

d	c_i	a_0	a_1	a_2	a_3	a_4	a_5
1	lin	1.50	4.20	—	—	—	—
	LP	1.50	4.20	—	—	—	—
2	lin	1.50	0.65	3.73	—	—	—
	LP	1.50	0.91	3.83	—	—	—
3	lin	1.50	2.04	0.53	2.18	—	—
	LP	1.50	1.91	0.62	2.23	—	—
4	lin	1.50	1.70	1.80	0.29	0.95	—
	LP	1.50	1.73	1.73	0.32	0.97	—
5	lin	1.50	1.76	1.48	1.06	0.13	0.33
	LP	1.50	1.75	1.50	1.03	0.13	0.34

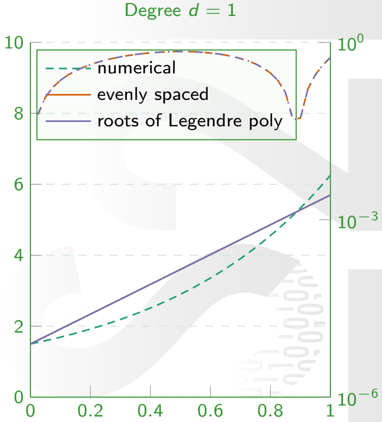

Generic First-Order ODE Collocation

Collocation

Assume we want to find the solution for

$$y' = f(t, y)\,, \qquad y(0) = y_0\,.$$

on the interval $t \in [0, 1]$ with the collocation polynomial

$$u(t) = \sum_{i=0}^{d} a_i\, t^i = \left[1, t, \ldots, t^d\right]\, \alpha = \tau^\top \alpha\,.$$

In addition, we have

$$u'(t) = \left[0, 1, t, \ldots, d\, t^{d-1}\right]\, \alpha = {\tau'}^\top\, \alpha\,,$$

Collocation method requires satisfying

$$u(0) = y(0) = y_0\,,$$
$$u'(t_0 + c_i) = f(t_0 + c_i, u(t_0 + c_i))\,,$$

at all *inner collocation points* $0 \leq c_1 < \cdots < c_i < \cdots < c_d \leq 1$. Substituting $u' = {\tau'}^\top\, \alpha$ yields

$$\begin{bmatrix} \tau^\top(t_0) \\ {\tau'}^\top(t_0 + c_1) \\ \vdots \\ {\tau'}^\top(t_0 + c_d) \end{bmatrix} \alpha = \begin{bmatrix} y_0 \\ f(t_0 + c_1, u(t_0 + c_1)) \\ \vdots \\ f(t_0 + c_d, u(t_0 + c_d)) \end{bmatrix}$$

which are $1 + d$ equations for the $d + 1$ unknowns of $u(t)$, respectively of α.

How to Use the Collocation Method

Collocation

To use the collocation method, a few facts have to be considered

- collocation function must satisfy the initial value
- collocation points must be well-chosen
  - polynomial: roots of shifted Legendre polynomial
  - splines: knots of Greville abscissae
- Choose between global or piecewise collocation
  - Piecewise reduces degree of local polynomial
  - Continuity of collocation function between intervals must be satisfied

To solve the ODE

$$y' = f(t, y)\,, \qquad y(t_0) = y_0\,,$$

remember that the *collocation function* $u(t)$ must satisfy

$$\begin{aligned} u(t_0) &= y_0\,. \\ u'(t_0 + c_i\,h) &= f(t_0 + c_i\,h, u(t_0 + c_i\,h))\,, \end{aligned}$$

at all *inner collocation points* $t_0 + c_i\,h$.
The resulting system of (non)linear equations can be solved with Newton-Raphson, Levenberg-Marquardt, etc.

Collocation Method vs. Numerical Integrators

Collocation Method

1. Requires more preparative work
2. Continuous solution of the IVP even between integration points
3. Interpolates the solution between t_n and t_{n+1}
4. Readily applicable to higher-order ODE
5. In principle applicable to any ODE/IVP
6. Transforms differential equation(s) into algebraic equation(s) (Can allow to define Jacobian in analytical form)
7. Comes in global and piecewise collocation (depending on collocation function)

Numerical Integrators

1. Only needs the ODE/IVP
2. Discretizes solution snap shots at integration points
3. Extrapolates solution from t_n to t_{n+1}
4. Needs state-reduction into first-order ODE
5. Handling of stiff ODEs is tricky

Section 6

Isogeometric Collocated Rod

Overview

Isogeometric Collocated Rod

Remember we *discretized* the centerline position and quaternion using p-th order NURBS as *shape functions* $\Pi_i(s)$

$$\boldsymbol{p}(s) = \sum_i^n \Pi_i(s)\, \boldsymbol{p}_i = \boldsymbol{\Pi}(s)\, \boldsymbol{P}_{\boldsymbol{p}} \;, \qquad \boldsymbol{q}(s) = \sum_i^n \Pi_i(s)\, \boldsymbol{q}_i = \boldsymbol{\Pi}(s)\, \boldsymbol{P}_{\boldsymbol{q}} \;.$$

Weeger, Yeung, and Dunn will rigorously substitute these into the kinematics and equilibrium equations, then use the collocation method to solve the resulting equilibrium ODE [6].

Strain measures

$$\boldsymbol{\varepsilon} = \boldsymbol{R}^\top \boldsymbol{p}' - \hat{\boldsymbol{e}}_3 \;,$$

$$\boldsymbol{\kappa} = \begin{bmatrix} \langle \boldsymbol{d}_2', \boldsymbol{d}_3 \rangle \\ \langle \boldsymbol{d}_3', \boldsymbol{d}_1 \rangle \\ \langle \boldsymbol{d}_1', \boldsymbol{d}_2 \rangle \end{bmatrix} \;.$$

Internal forces

$$\boldsymbol{n} = \boldsymbol{R}\,\boldsymbol{\sigma} = \boldsymbol{R}\,\boldsymbol{K}_{\text{SE}}(\boldsymbol{\varepsilon} - \boldsymbol{\varepsilon}_0) \;,$$

$$\boldsymbol{m} = \boldsymbol{R}\,\boldsymbol{\chi} = \boldsymbol{R}\,\boldsymbol{K}_{\text{BT}}(\boldsymbol{\kappa} - \boldsymbol{\kappa}_0) \;.$$

Equilibrium equations

$$\boldsymbol{n}' + \hat{\boldsymbol{n}} = \mathbb{0} \;,$$

$$\boldsymbol{m}' + \boldsymbol{p}' \times \boldsymbol{n} + \hat{\boldsymbol{m}} = \mathbb{0} \;.$$

Strong Collocation of the Equilibrium

Isogeometric Collocated Rod

Application of *collocation of the strong form* to the equilibrium equations requires them to be *evaluated at the collocation points* τ_i, $i = 1, \ldots, n$. For *internal collocation* points τ_i, $i = 2, \ldots, n-1$, this yields

$$\begin{aligned} \boldsymbol{e}_n(\tau_i) &= \boldsymbol{n}'(\tau_i) + \hat{\boldsymbol{n}}(\tau_i) = \mathbb{0}\,, \\ \boldsymbol{e}_m(\tau_i) &= \boldsymbol{m}'(\tau_i) + \boldsymbol{p}'(\tau_i) \times \boldsymbol{n}(\tau_i) + \hat{\boldsymbol{m}}(\tau_i) = \mathbb{0}\,, \\ \boldsymbol{e}_{\boldsymbol{q}}(\tau_i) &= \langle \boldsymbol{q}(\tau_i), \boldsymbol{q}(\tau_i) \rangle - 1 = 0\,. \end{aligned}$$

At the *boundaries* i.e., $\tau_1 = 0$ and $\tau_n = 1$, we have

Dirichlet-type conditions

$$\begin{aligned} \boldsymbol{e}_n(\tau_i) &= \boldsymbol{n}(\tau_i) - \overline{\boldsymbol{n}}(\tau_i) = \mathbb{0}\,, \\ \boldsymbol{e}_m(\tau_i) &= \boldsymbol{m}(\tau_i) - \overline{\boldsymbol{m}}(\tau_i) = \mathbb{0}\,, \\ \boldsymbol{e}_{\boldsymbol{q}} &= \langle \boldsymbol{q}(\tau_i), \boldsymbol{q}(\tau_i) \rangle - 1 = \mathbb{0}\,. \end{aligned}$$

Neumann-type conditions

$$\begin{aligned} \boldsymbol{e}_{\boldsymbol{p}}(\tau_i) &= \boldsymbol{p}(\tau_i) - \overline{\boldsymbol{p}}(\tau_i) = \mathbb{0}\,, \\ \boldsymbol{e}_{\boldsymbol{q}}(\tau_i) &= \boldsymbol{q}(\tau_i) - \overline{\boldsymbol{q}}(\tau_i) = \mathbb{0}\,. \end{aligned}$$

Strong Collocation of the Equilibrium

Isogeometric Collocated Rod

With internal forces and moments

$$\boldsymbol{n} = \boldsymbol{R}\,\boldsymbol{\sigma} = \boldsymbol{R}\,\boldsymbol{K}_{\text{SE}}(\boldsymbol{\varepsilon} - \boldsymbol{\varepsilon}_0)\,, \qquad \boldsymbol{m} = \boldsymbol{R}\,\boldsymbol{\chi} = \boldsymbol{R}\,\boldsymbol{K}_{\text{BT}}(\boldsymbol{\kappa} - \boldsymbol{\kappa}_0)\,,$$

their spatial derivatives read

$$\begin{aligned}
\boldsymbol{n}' &= \boldsymbol{R}'\,\boldsymbol{\sigma} + \boldsymbol{R}\,\boldsymbol{\sigma}' \\
&= \boldsymbol{R}'\,\boldsymbol{K}_{\text{SE}}(\boldsymbol{\varepsilon} - \boldsymbol{\varepsilon}_0) + \boldsymbol{R}\,\boldsymbol{K}_{\text{SE}}(\boldsymbol{\varepsilon}' - \boldsymbol{\varepsilon}_0') \\
&= \boldsymbol{R}'\,\boldsymbol{K}_{\text{SE}}\left(\boldsymbol{R}^\top\boldsymbol{p}' - \hat{\boldsymbol{e}}_3 - \boldsymbol{\varepsilon}_0\right) + \boldsymbol{R}\,\boldsymbol{K}_{\text{SE}}\left(\boldsymbol{R}'^\top\boldsymbol{p}' + \boldsymbol{R}^\top\boldsymbol{p}'' - \boldsymbol{\varepsilon}_0'\right)\,, \\
\boldsymbol{m}' + \boldsymbol{p}' \times \boldsymbol{n} &= \boldsymbol{R}'\,\boldsymbol{\chi} + \boldsymbol{R}\,\boldsymbol{\chi}' + \boldsymbol{p}' \times (\boldsymbol{R}\,\boldsymbol{\sigma}) \\
&= \boldsymbol{R}'\,\boldsymbol{K}_{\text{BT}}(\boldsymbol{\kappa} - \boldsymbol{\kappa}_0) + \boldsymbol{R}\,\boldsymbol{K}_{\text{BT}}(\boldsymbol{\kappa}' - \boldsymbol{\kappa}_0') + \boldsymbol{p}' \times \left(\boldsymbol{R}\,\boldsymbol{K}_{\text{SE}}\left(\boldsymbol{R}^\top\boldsymbol{p}' - \hat{\boldsymbol{e}}_3 - \boldsymbol{\varepsilon}_0\right)\right)\,,
\end{aligned}$$

which we can *readily plug* into the *strong form of the collocation method* and solve for the *unknown control points* $\boldsymbol{P}_{\boldsymbol{p}}$ and $\boldsymbol{P}_{\boldsymbol{q}}$.

Mixed Isogeometric Collocation Method

Isogeometric Collocated Rod

Due to *shear locking* (decreasing thickness of a beam), the convergence of the numerical discretization method deteriorates. Thus, a *mixed collocation method* was developed.

In addition to using NURBS for centerline position $\boldsymbol{p}$ and quaternions $\boldsymbol{q}$, the *internal forces* and *internal moments* are also *being discretized* likewise:

$$\boldsymbol{n}_{\mathrm{d}}(s) = \sum_{i}^{n} \Pi_i(s)\, \boldsymbol{n}_i = \boldsymbol{\Pi}(s)\, \boldsymbol{P}_{\boldsymbol{n}} \,, \qquad \boldsymbol{m}(s) = \sum_{i}^{n} \Pi_i(s)\, \boldsymbol{m}_i = \boldsymbol{\Pi}(s)\, \boldsymbol{P}_{\boldsymbol{m}} \,,$$

This yields the collocated equations at internal collocation points τ_i, $i = 2, \ldots, n-1$

$$\begin{aligned}
\boldsymbol{e}_n(\tau_i) &= \boldsymbol{n}_{\mathrm{d}}'(\tau_i) + \hat{\boldsymbol{n}}(\tau_i) = \mathbb{O}\,, \\
\boldsymbol{e}_m(\tau_i) &= \boldsymbol{m}_{\mathrm{d}}'(\tau_i) + \boldsymbol{p}_{\mathrm{d}}(\tau_i) \times \boldsymbol{n}_{\mathrm{d}}(\tau_i) + \hat{\boldsymbol{m}}(\tau_i)\,, \\
\boldsymbol{e}_{\boldsymbol{q}}(\tau_i) &= \langle \boldsymbol{q}_{\mathrm{d}}(\tau_i), \boldsymbol{q}_{\mathrm{d}}(\tau_i) \rangle - 1 = 0\,, \\
\boldsymbol{e}_{\mathrm{u}} &= \boldsymbol{n}_{\mathrm{d}}(\tau_i) - (\boldsymbol{R}\,\boldsymbol{\sigma})(\tau_i) = \mathbb{O}\,, \\
\boldsymbol{e}_{\chi} &= \boldsymbol{m}_{\mathrm{d}}(\tau_i) - (\boldsymbol{R}\,\chi)(\tau_i) = \mathbb{O}\,.
\end{aligned}$$

Primal vs. Mixed Collocation Method [6]

Isogeometric Collocated Rod

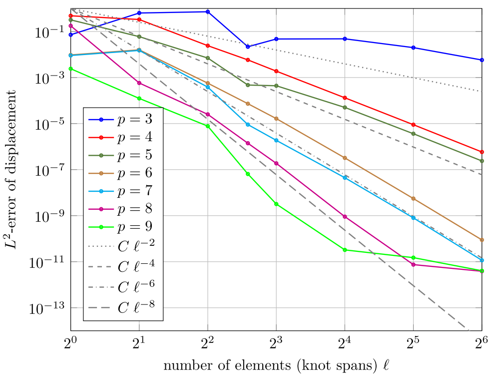

Figure: Thickness $t = 0.1$, primal formulation $(\boldsymbol{p}_d, \boldsymbol{q}_d)$.

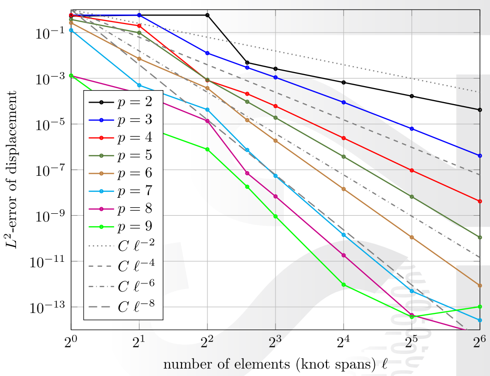

Figure: Thickness $t = 0.1$, mixed formulation $(\boldsymbol{p}_d, \boldsymbol{q}_d, \boldsymbol{n}_d, \boldsymbol{m}_d)$.

Primal vs. Mixed Collocation Method [6]

Isogeometric Collocated Rod

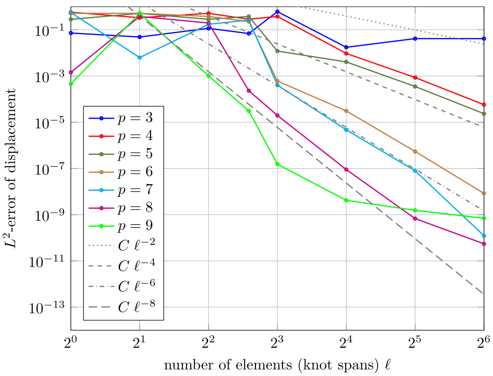

Figure: Thickness $t = 0.01$, primal formulation $(\boldsymbol{p}_\mathrm{d}, \boldsymbol{q}_\mathrm{d})$.

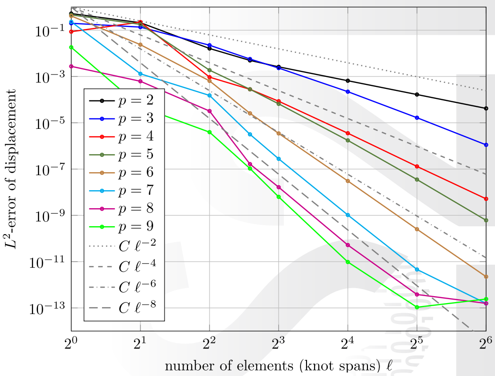

Figure: Thickness $t = 0.01$, mixed formulation $(\boldsymbol{p}_\mathrm{d}, \boldsymbol{q}_\mathrm{d}, \boldsymbol{n}_\mathrm{d}, \boldsymbol{m}_\mathrm{d})$.

Helical Spring Displacement [6]

Isogeometric Collocated Rod

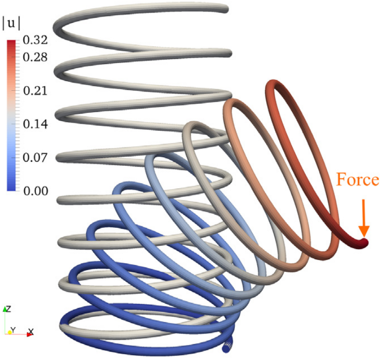

Figure: Initial configuration of helical spring and roll-up.

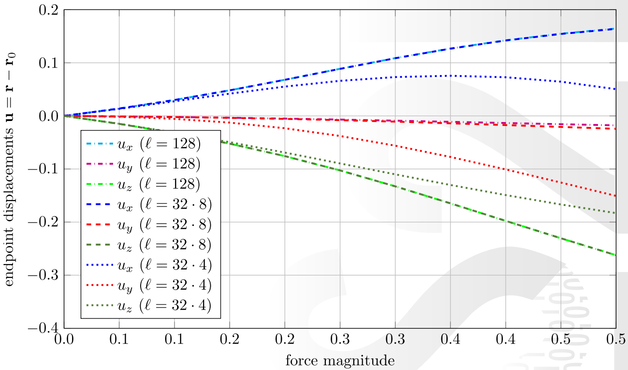

Figure: End-point displacement when subject to different end forces for different basis functions.

Section 7

Closing

Today I Learned

- We can describe the deformation field of a Cosserat rod using NURBS as basis/shape functions
- With isogeometric analysis and collocation method, the ODE is transformed to a system of nonlinear algebraic equations
- These methods have been carefully studied before and validated in numerical applications
- The presented method is a promising alternative to existing discretization methods for Cosserat rods

References

[1] O. Altuzarra, D. Caballero, Q. Zhang, and F. J. Campa, "Kinematic characteristics of parallel continuum mechanisms," in *Advances in Robot Kinematics 2018*, ser. Springer Proceedings in Advanced Robotics, J. Lenarcic and V. Parenti-Castelli, Eds., vol. 8, Cham: Springer International Publishing, 2019, pp. 293–301, ISBN: 978-3-319-93187-6. DOI: 10.1007/978-3-319-93188-3_34.

[2] C. B. Black, J. Till, and D. C. Rucker, "Parallel continuum robots, Modeling, analysis, and actuation-based force sensing," *IEEE Transactions on Robotics*, vol. 34, no. 1, pp. 29–47, Feb. 1, 2018, ISSN: 1552-3098. DOI: 10.1109/TRO.2017.2753829.

[3] F. J. Campa, M. Diez, D. Diaz-Caneja, and O. Altuzarra, "A 2 dof continuum parallel robot for pick & place collaborative tasks," in *Advances in Mechanism and Machine Science*, ser. Mechanisms and Machine Science, T. Uhl, Ed., vol. 73, Cham: Springer International Publishing, 2019, pp. 1979–1988, ISBN: 978-3-030-20130-2. DOI: 10.1007/978-3-030-20131-9_196.

[4] J. Till and D. C. Rucker, "Elastic Stability of Cosserat Rods and Parallel Continuum Robots," *IEEE Transactions on Robotics*, vol. 33, no. 3, pp. 718–733, 2017, ISSN: 1552-3098. DOI: 10.1109/TRO.2017.2664879.

References

[5] T. J. R. Hughes, J. A. Cottrell, and Y. Bazilevs, "Isogeometric analysis, Cad, finite elements, nurbs, exact geometry and mesh refinement," *Computer Methods in Applied Mechanics and Engineering*, vol. 194, no. 39, pp. 4135–4195, 2005, ISSN: 0045-7825. DOI: 10.1016/j.cma.2004.10.008.

[6] O. Weeger, S.-K. Yeung, and M. L. Dunn, "Isogeometric collocation methods for Cosserat rods and rod structures," *Computer Methods in Applied Mechanics and Engineering*, vol. 316, pp. 100–122, 2017, PII: S004578251630336X, ISSN: 0045-7825. DOI: 10.1016/j.cma.2016.05.009. (visited on 05/20/2020).

EOF